ISSN 1023-1935, Russian Journal of Electrochemistry, 2020, Vol. 56, No. 2, pp. 124–131. © Pleiades Publishing, Ltd., 2020.
Russian Text © The Author(s), 2020, published in Elektrokhimiya, 2020, Vol. 56, No. 2, pp. 133–140.

Layered Solid-Electrolyte Membranes Based on Zirconia: Production Technology[1]

O. Yu. Zadorozhnaya[a], *, E. A. Agarkova[b], O. V. Tiunova[c], and Yu. K. Napochatov[a]

[a] *NEVZ-CERAMICS, Novosibirsk, 630049 Russia*

[b] *Moscow Institute of Physics and Technology (National Research University), Dolgoprudnyi, Moscow oblast, 117303 Russia*

[c] *Tomsk Polytechnic University, Tomsk, 634050 Russia*

**e-mail: olgazador@mail.ru*

Received December 25, 2018; revised March 12, 2019; accepted June 13, 2019

Abstract—A solid electrolyte membrane is a key part of a solid oxide fuel cell (SOFC). This paper presents the results of our study of the effects of particle size of the starting powders, composition of organic additives in suspension, and process parameters on the quality of three-layer ceramic sheets of solid electrolyte with dimensions of 100 × 100 mm and a thickness of 0.15 mm, made by casting on a moving tape. The inner layer was 10Sc1YSZ (10 mol % Sc_2O_3, 1 mol % Y_2O_3, 89 mol % ZrO_2)—a material with the highest oxygen ion conductivity among zirconia-based solid solutions. 6ScSZ was chosen for the outer layers (6 mol % Sc_2O_3, 94 mol % ZrO_2). The three-layer architecture of the solid electrolyte membranes allows the improvement of the mechanical characteristics while maintaining the required functional properties (primarily, anion conductivity). This study is devoted to optimization of the production technology of these layered membranes by tape casting.

Keywords: solid oxide fuel cells, supporting electrolyte, tape casting, 6ScSZ, 10Sc1YSZ, microstructure

DOI: 10.1134/S1023193520020123

INTRODUCTION

Solid oxide fuel cells (SOFCs) are energy conversion devices capable of generating electricity with high efficiency (up to 60% electric efficiency and 90% including thermal efficiency) and are considered one of the key technologies for the future hydrogen energy economy. The electrolytes of the currently produced SOFCs consist of yttria (YSZ) and/or scandia (ScSZ) stabilized zirconia because these materials have high ion conductivity and excellent chemical, thermal, and mechanical stability. In addition to these characteristics, the electrolyte should be gas-tight, with a density higher than 94–95% of theoretical. In the production of planar SOFCs, tape casting is the most widely used method for the production of thin plates because this technology affords ceramic sheets with controlled thickness and large area. Earlier, we reported the results on the manufacture of single-layer membranes 200–250 μm thick by this method [1]. Tape casting affords SOFC components of electrolyte- and anode-supporting structures [2–5] with thicknesses of 0.01–1.5 mm [6–8].

One of the most important factors in tape casting is the composition of the casting slurry, which affects the characteristics of both unannealed and sintered tapes. The main requirements for the casting slurry for tape casting are as follows:

—high content of the solid phase to form a strong tape during casting and drying;

—the absence of particle agglomerates and the optimum particle size distribution of ceramic powder to obtain a uniform tape;

—rheological properties, due to which the tape is obtained without defects.

The unsintered tapes are laminated to increase the thickness of the electrolyte and form a multilayer structure [9, 10]. The characteristics of the sintered plates also depend on the sintering conditions: rate, temperature, exposure time at the maximum temperature, and load applied during the sintering [11–13].

The goal of this study was to investigate the key parameters at various stages of the manufacture of solid electrolyte plates on the properties of the final plates and to evaluate the optimum particle size composition of the powders, the composition of the casting slurry, and the technological parameters that allow mass production of solid electrolyte plates with dimensions of 100 × 100 × 0.15 mm for SOFCs. The three-layer structure of the manufactured membranes was patented previously [14].

[1] Published on the basis of materials of the 5th All-Russia Conference "Fuel Cells and Power Plants Based on Them" (with international participation), Suzdal, 2018.

EXPERIMENTAL

Powders of zirconia stabilized with scandia 6ScSZ (94 mol % ZrO_2 + 6 mol % Sc_2O_3) and with scandia and yttria 10Sc1YZ (89 mol % ZrO_2 + 10 mol % Sc_2O_3 + 1 mol % Y_2O_3) (Neokhim, Russia) were used.

The process flow diagram for the preparation of three-layer sandwich plates of solid electrolyte for SOFCs is presented in Fig. 1. At the first stage of slurry preparation, the starting 6ScSZ or 10Sc1YSZ powder was ground with zirconia balls (diameter 10 mm) in a polyethylene drum with a solvent, which was an azeotropic mixture of methyl ethyl ketone (chemically pure grade), mass fraction of the main substance at least 99.5%) and propanol-1 (reagent grade), mass fraction of the main substance at least 99.5%). Menhaden Fish Oil (Sigma, United States) was used as a dispersant. To determine the dynamics of grinding and assess the changes in the particle size distribution, the 6ScSZ powder was ground for 24 and 44 h at a mass ratio of material : balls : solvents = 2 : 5 : 1. After 24 h of grinding, plasticizers were introduced in the resulting suspension: polyethylene glycol PEG -2000 (Sigma-Aldrich, United States), Santicizer (Valtris Specialty Chemicals, United States), and Butvar polyvinyl butyral binder (Showiningan, England). Then the mixture was stirred for 24 h, and the resulting slurry was separated from the balls and degassed for 6–12 h at a rate of up to 10 rpm.

The optimum composition of organic additives in the slurry was chosen based on the characteristics of the ceramic tape obtained after drying, such as homogeneous microstructure, the absence of macroscopic defects, and ease of separation from the support film after drying to prevent tensile stresses during tape removal. For this purpose, four compositions (R1–R4, Table 1) were developed, which differed in the amount of solvents and the ratio and amount of plasticizers. The ratio of plasticizers Santicizer : PEG-2000 was 70 : 30 vol % in R1 and 55 : 45 vol % in R2. The composition of R3 differed from that of R2 in the amount of plasticizers, increased by 6% at the same ratio. R4 was a composite with a reduced amount of plasticizers at Santicizer : PEG-2000 = 50 : 50 vol % for casting on a polyethylene terephthalate (PET) film with a silicone coating.

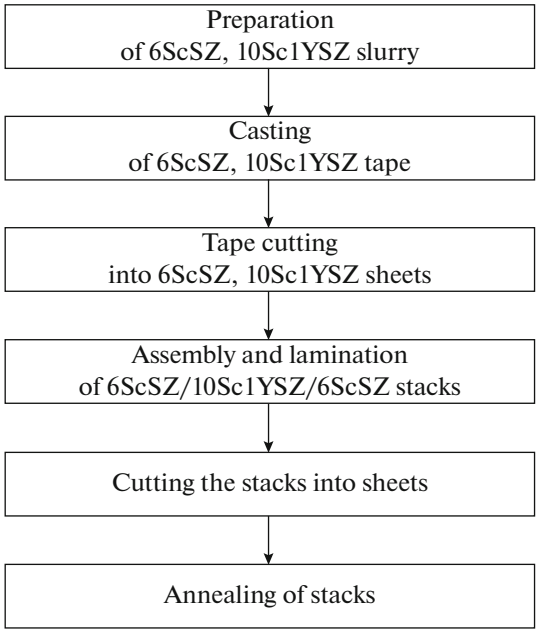

Fig. 1. Process flow diagram for the preparation of three-layer sandwich plates by tape casting.

The casting and drying of the 6ScSZ and 10Sc1YSZ ceramic tapes were performed on a unit of the KEKO line (Slovenia) at 20–22°C using a PET support film with a silicone coating or without coating depending on the composition of the organic additions in the slurry (Table 1).

The tapes were cut into sheets on an SC-25MNC unit for cutting ceramic sheets (KEKO, Slovenia). The 6ScSZ/10Sc1YSZ/6ScSZ stacks were laminated using an ILS-66 isostatic lamination system (KEKO, Slovenia) at a maximum pressure of 30–40 MPa and a tem-

Table 1. Formulations of casting slurries for 10Sc1YSZ tape casting

Component name	Function of component	Content, vol %			
		R1 composite	R2 composite	R3 composite	R4 composite
10Sc1YSZ powder	Ceramic powder	18.4	18.3	19.3	19.5
Methyl ethyl ketone	Solvent	43.5	43.2	41.7	44.5
Isopropanol	Solvent	19.7	19.6	19.1	20.2
Fish oil	Dispersing agent	1.9	1.9	2.0	2.0
Santisizer	Plasticizer	5.9	4.9	5.2	2.8
PEG-2000	Plasticizer	2.6	4.1	4.3	2.8
Polyvinyl butyral	Binder	8.0	8.0	8.4	8.2
Type of support film	–	Uncoated PET	Uncoated PET	Uncoated PET	PET with a silicone coating

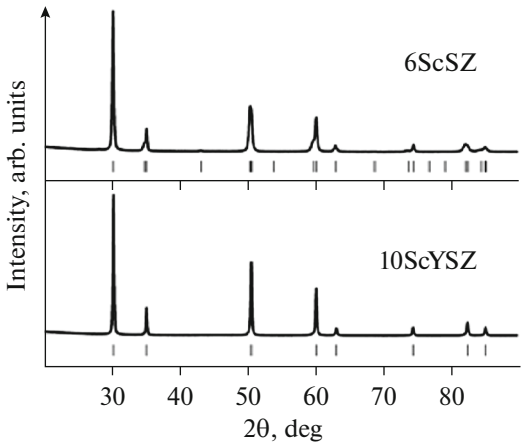

Fig. 2. Diffraction patterns of the 6ScSZ and 10Sc1YSZ powders.

perature of 50–70°C. The cutting into sheets was performed on an SM-15 automatic cutting machine (KEKO, Slovenia). The resulting sheets were annealed on porous alumina fireproof tiles in a Nabertherm 276 high-temperature chamber furnace (Germany) to a maximum temperature of 1500°C at a holding time of 1.5 h. The load from the load tile was 1.7 g/cm^2 of the sheet area.

The average particle size of ceramic powders was determined by laser diffraction on an Analysette 22 NanoTec plus analyzer (Fritsch, Germany). The specific surface area of the powders was analyzed by the low-temperature nitrogen adsorption-desorption method on a Sorbtometr analyzer (Katakon, Russia). The micrographs of the powders and ceramic samples were obtained using JSM-6010 LA (Jeol, Japan) and Supra 50vp (Carl Zeiss, Germany) scanning electron microscopes. The viscosity of the slurries was measured on a Brookfield DV-I Prime rotational viscosimeter (Brookfield Engineering Laboratories, United States).

The apparent density and water absorption of the samples after annealing were determined by hydrostatic weighing according to GOST (State Standard) 24409–80.

The X-ray powder diffraction patterns were recorded using a Siemens D-500 diffractometer (Cu$K\alpha_1$ radiation) in the range of angles $2\theta = 20°–135°$.

RESULTS AND DISCUSSION

An analysis of the diffraction patterns of the starting powders (Fig. 2) showed that the tetragonal phase was the main phase of the 6ScSZ powder. The low-intensity reflection at a reflection angle of 28.3° indicated the presence of traces of impurity. The 10Sc1YSZ powder is represented only by the cubic phase. The average crystallite size evaluated by the Scherrer formula was 95 nm for 6ScSZ and 170 nm for 10Sc1YSZ. The micrographs of the starting 6ScSZ and 10Sc1YSZ powders are shown in Figs. 3a and 3b, respectively.

According to the description of the starting powders given by the manufacturer, they were thermally treated at 1000°C for 2 h to improve the technological properties after their synthesis. Table 2 gives the main characteristics of the 6ScSZ and 10Sc1YSZ starting powders. Figure 4 shows the particle size distribution curves of the 10Sc1YSZ powder. According to Table 2 and Figs. 3b and 4, the 10Sc1YSZ powder does not contain agglomerates of particles larger than 2 μm; the particles are nearly spherical; $d_{50} = 0.7$ μm, $d_{90} = 1.3$ μm; the particle size distribution is monomodal. This particle distribution does not lead to a dense packing of particles during the preparation of the slurry because the voids between the particles are filled with the solvents, resulting in increased viscosity. On the other hand, the monomodal particle size distribution leads to the formation of a more uniform structure during the sintering of ceramics because the anisotropy of the

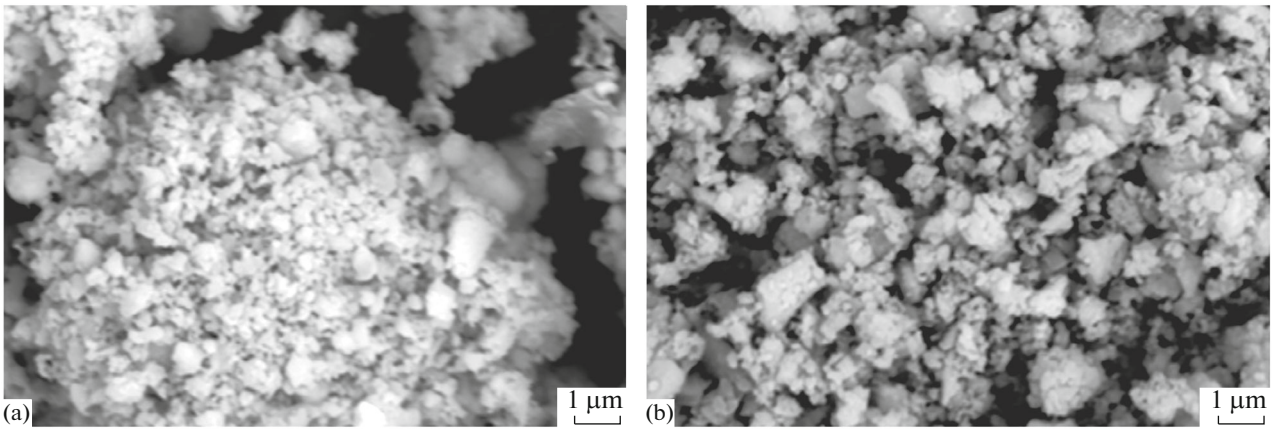

Fig. 3. Micrographs of the starting (a) 6ScSZ and (b) 10Sc1YSZ powders.

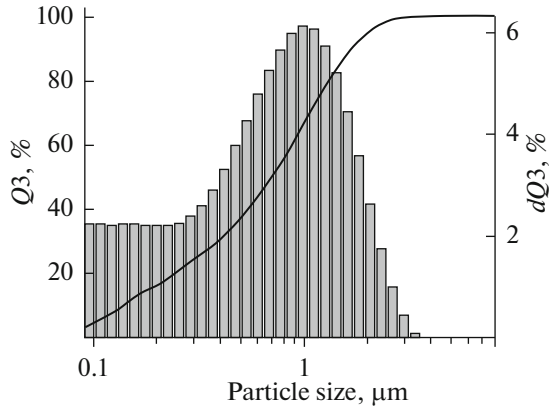

Fig. 4. Particle size distribution of the starting 10Sc1YSZ powder.

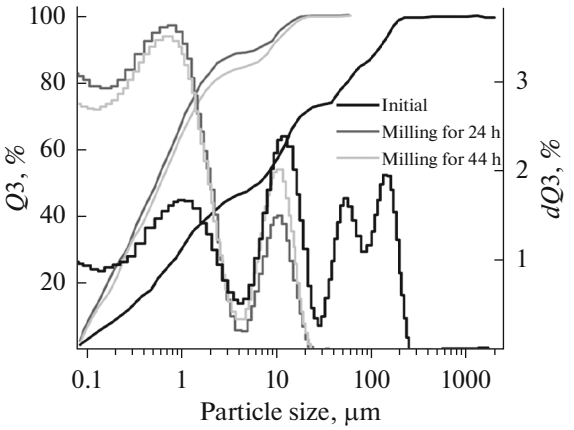

Fig. 5. Particle size distribution of the starting 6ScSZ powder and the powders after grinding for 24 and 44 h.

shrinkage coefficient and anomalous grain growth are not observed [15].

The integral and differential particle size distributions of the 6ScSZ powder before and after wet grinding for 24 and 44 h are shown in Fig. 5. The starting powder (d_{50} = 7.0 μm, d_{90} = 123.6 μm) has a multimodal particle size distribution and contains large agglomerates that decompose during the grinding for 24 h to d_{50} = 0.6 μm, d_{90} = 6.7 μm; the particle size distribution of the powder is bimodal. Further grinding

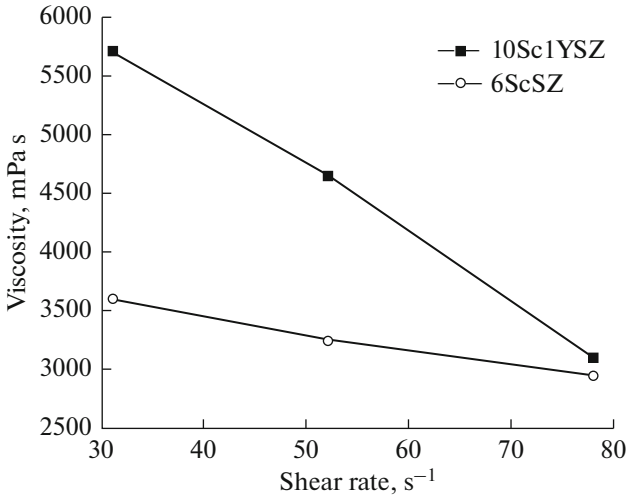

Fig. 6. Dependence of the viscosity of the 6ScSZ and 10Sc1YSZ slurries on the shear rate.

up to 44 h does not lead to any noticeable change in the particle size distribution. Therefore, it is necessary to lower the calcination temperature of 6ScSZ because of the formation of large and stable agglomerates of the powder at 1000°C, which do not decompose to d_{90} of less than 2 μm even after 44 h of grinding. The presence of agglomerated grains at the stage of ceramic sintering leads to irregular microstructure and nonuniform shrinkage.

Figure 6 shows the dependences of the viscosity of the 6ScSZ and 10Sc1YSZ slurries prepared according to R1 on the shear rate. The slurries exhibit pseudoplastic behavior, with the viscosity decreasing at increased shear rates. The micrographs of the structure of tapes from 6ScSZ and 10Sc1YSZ slurries prepared according to the R1 formulation are shown in Fig. 7. The presence of agglomerates that were not destroyed after grinding in the 6ScSZ powder led to an irregular structure of the tape and the appearance of pores with sizes of up to 2 μm.

The absence of large agglomerates and the monomodal particle size distribution of 10Sc1YSZ leads to a more uniform structure of the cast tape regardless of the composition of the slurry. The micrographs of the 10Sc1YSZ tapes obtained from the slurries of R1–R4 compositions are shown in Fig. 8. The ratio of organic

Table 2. Characteristics of the starting 6ScSZ and 10Sc1YSZ powders

Powder	Particle size distribution, μm			S_{sp}, m^2/g	Moisture, %
	d_{10}	d_{50}	d_{90}		
6ScSZ	0.2	7.0	123.6	5.19	0.19
10Sc1YSZ	0.4	0.7	1.3	4.9	0.18

d_{10}, d_{50}, and d_{90} is the limiting diameter for 10, 50, and 90% of all particles, respectively. S_{sp} is the specific surface area of particles.

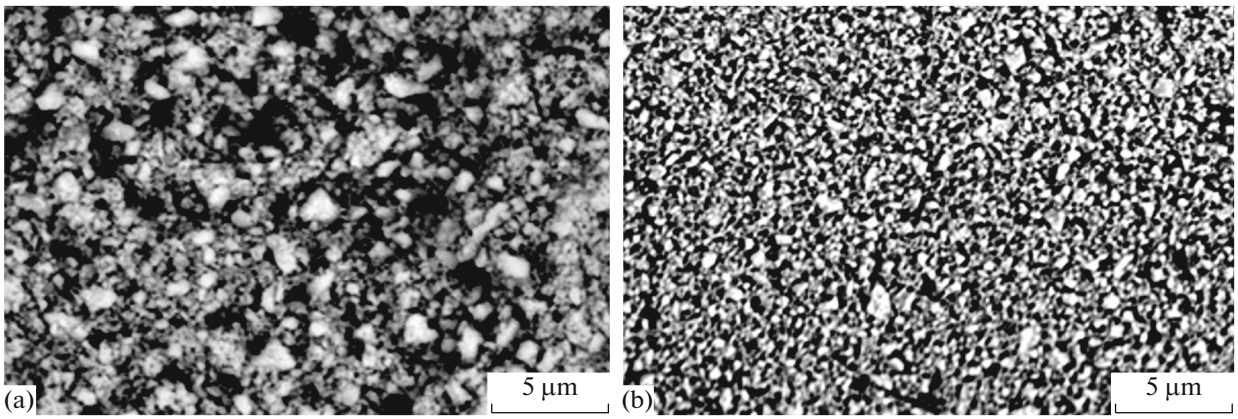

Fig. 7. Micrographs of the structure of the (a) 6ScSZ (a) and (b) 10Sc1YSZ tapes prepared from slurries of the R1 formulation.

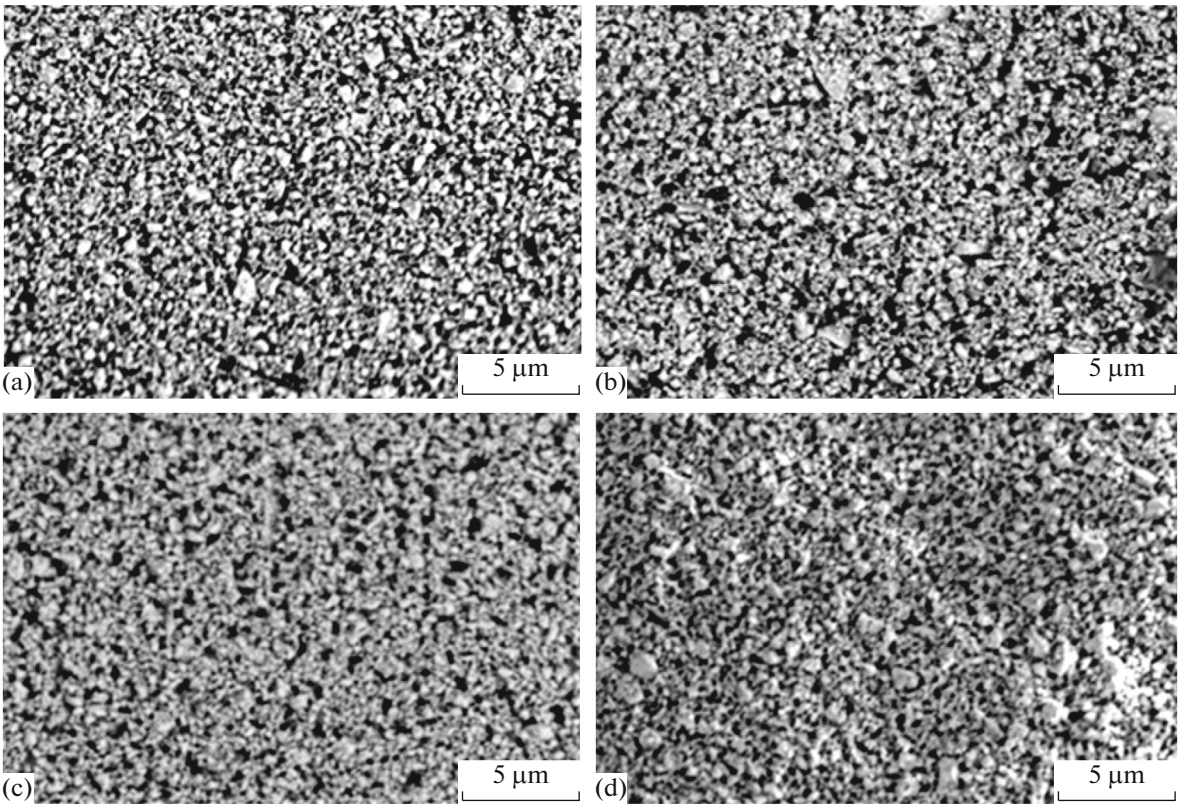

Fig. 8. SEM image of the 10Sc1YSZ tape prepared from the slurries of (a) R1, (b) R2, (c) R3, and (d) R4 compositions.

components in the slurry based on the 10Sc1YSZ powder significantly affected the tape separation from the support film. Table 3 shows the properties of the tapes obtained from the 10Sc1YSZ-based slurries prepared according to R1–R4 formulations.

The 10Sc1YSZ tapes cast from the slurries prepared according to the R3 and R4 formulations are shown in Fig. 9. The tape cast on the uncoated PET film had higher adhesion to the film and no wrinkling after drying. As a result of the analysis of the properties of the tapes obtained from the 10Sc1YSZ slurries with different proportions of organic components, a slurry with a composition of R3 was chosen for further work; this afforded a tape with a homogeneous microstructure and without defects, which was detached from the support PET film with little effort.

The cast 6ScSZ and 10Sc1YSZ tapes were cut for further lamination in an isostatic press. The obtained (6ScSZ/10Sc1YSZ/6ScSZ) three-layer stacks were annealed on porous alumina refractory plates to a

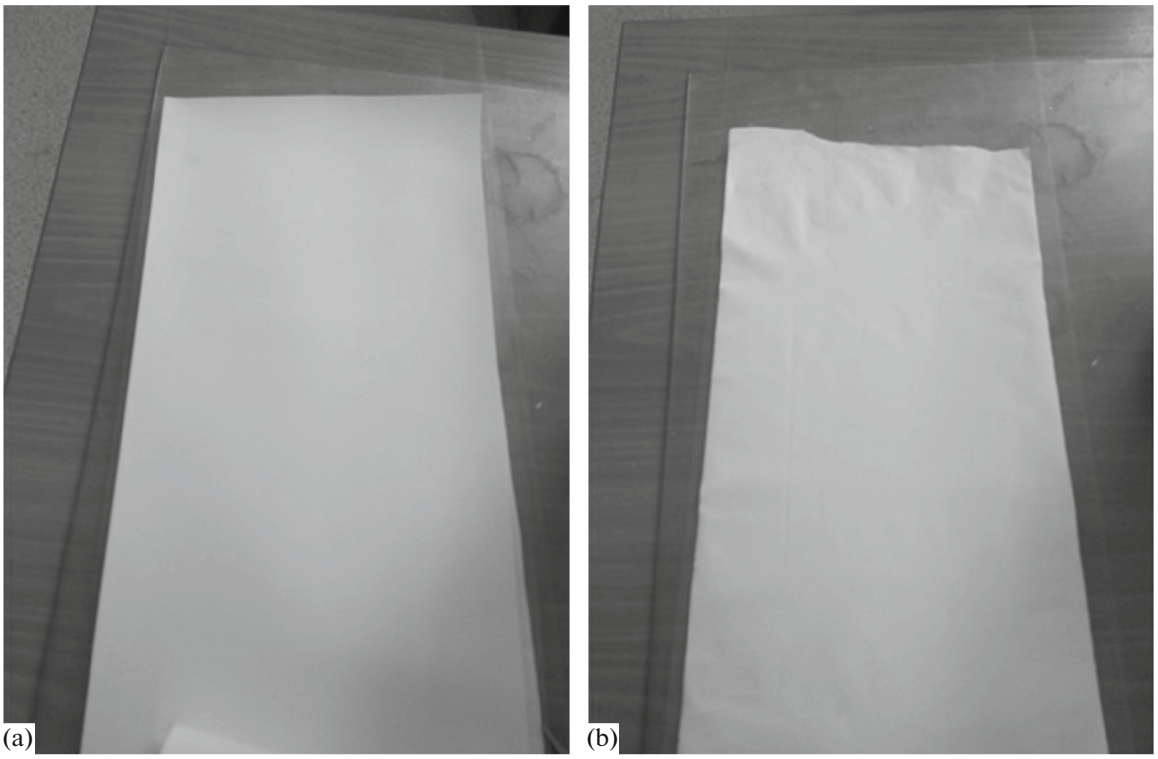

Fig. 9. 10Sc1YSZ tapes cast from the slurry of R3 formulation on an uncoated PET film (a) and (b) of R4 composition on a silicone-coated PET film.

maximum temperature of 1500°C with a holding time of 1.5 h. The plates were unpolished or polished refractory during the loading of sheets.

The sheets with dimensions of 100 × 100 × 0.15 mm obtained after their sintering on the unpolished and polished refractory plates are shown in Figs. 10a and 10b, respectively. The sheets annealed using the unpolished refractory plates have defects in the form of elongated or chipped corners. This is due to the deviation of the refractory plates from planarity and, as a result, to the local pressing of the ceramic sheet by the load plate to the base plate, which prevents the movement of certain sections of the sheet in the course of shrinkage during sintering. The sheets annealed on the polished refractory plates are smooth-faced and have no deviations from planarity and parallelism. The apparent density of the obtained sheets is 5.7 g/cm^3.

Figure 11 shows the microstructure of the surface and fracture of the 6ScSZ/10Sc1YSZ/6ScSZ sheet after sintering. The surface structure is homogeneous, the grain size of 6ScSZ does not exceed 3 μm. Some pores with a diameter of no more than 1 μm are present. The cross section of the sheet has a pronounced three-layer structure with thicknesses of 30 and 80 μm for the outer and inner layers, respectively. The micropores with a diameter of less than 1 μm that are present throughout the thickness of the sample do not form a connected system and should not have any significant effect on the transport or mechanical characteristics of the obtained sheets.

Table 3. Properties of tapes obtained from the 10Sc1YSZ slurry according to the R1–R4 formulations

Slurry composition	R1	R2	R3	R4
Quality of ceramic tape	No defects	No defects	No defects	Folds, partial disruptions
Tape separation from support film after drying	Separated with an effort	Separated with an effort, gets creased	Separated with a slight effort (Fig. 9a)	Separated with an effort during the drying (Fig. 9b)

Fig. 10. Sheets after annealing on the (a) unpolished plates (the characteristic stretching and chipping of corners are marked with red circles) and (b) polished plates (without visible defects).

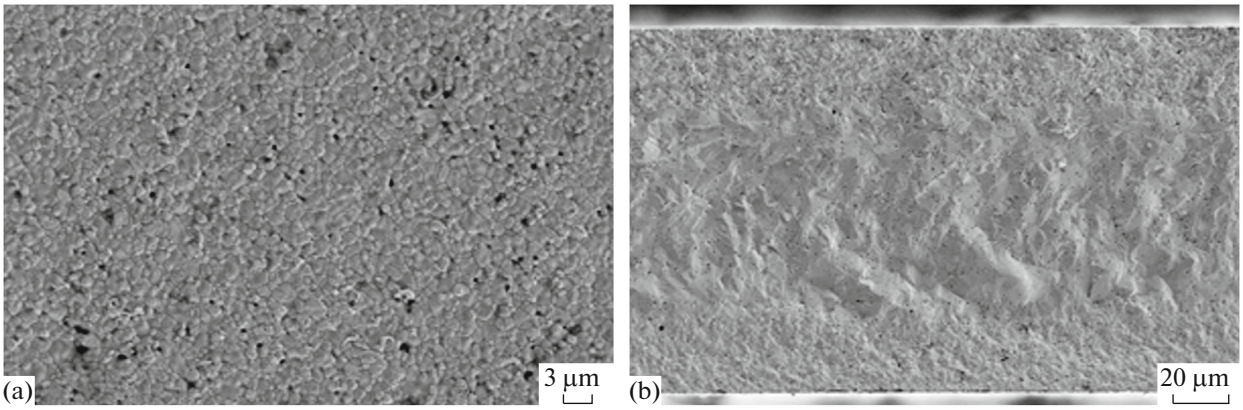

Fig. 11. Microstructure of the (a) end surface and (b) fracture surface of the 6ScSZ/10Sc1YSZ/6ScSZ sheet.

CONCLUSIONS

The results obtained by optimization of the technology for the preparation of zirconia-based layered solid electrolyte membranes by tape casting (on a moving tape) were presented. The membranes are intended for use in the production of planar solid oxide fuel cells with a supporting electrolyte. The membranes have dimensions 100 × 100 mm and a thickness of less than 150 μm. Their flexibility greatly simplifies the manufacture of fuel cells and batteries based on them. The membranes meet the geometry and microstructure requirements. The functional characteristics will be reported in our next publications.

FUNDING

This study was financially supported by the Russian Scientific Foundation (grant no. 17-79-30071 "Development of scientifically sound ways of optimization of the power

and weight and size characteristics of SOFC batteries of planar design and creation of a fuel processor for highly efficient transport and stationary power plants.")

CONFLICT OF INTEREST

The authors declare that they have no conflict of interest.

REFERENCES

1. Tiunova, O.V., Zadorozhnaya, O.Yu., Nepochatov, Yu.K., Burmistrov, I.N., Kuritsyna, I.E., and Bredikhin, S.I., Ceramic membranes based on scandium-stabilized ZrO_2 obtained by tape casting technique, *Russ. J. Electrochem.*, 2014, vol. 50, p. 719.
2. Minh, N.Q., Ceramic fuel cells, *J. Am. Ceram. Soc.*, 1993, vol. 76, p. 563.
3. Andujar, J.M. and Segura, F., Fuel cells: history and updating. A walk along two centuries, *Renewable Sustainable Energy Rev.*, 2009, vol. 13, p. 2309.
4. Ormerod, R.M., Solid oxide fuel cells, *Chem. Soc. Rev.*, 2003, vol. 32, p. 17.
5. Singhal, S.C. and Kendall, K., *High-Temperature Solid Oxide Fuel Cells: Fundamentals, Design and Applications*, Oxford: Elsevier, 2003, p. 424.
6. Cheng, J.G., Fu, Q.X., Liu, X.Q., et al., *Key Eng. Mater.*, 2202, vols. 224–226, p. 173.
7. Fu, C.J., Chan, S.H., Liu, Q.L., et al., *Int. J. Hydrogen Energy*, 2010, vol. 35, p. 301.
8. Costa, R., Hafsaoui, J., Almeida De Oliveira, A.P., et al., *J. Appl. Electrochem.*, 2009, vol. 39, p. 485.
9. Gurauskis, J., Sanchez-Herencia, A.J., and Baudin, C., Joining green ceramic tapes made from water-based slurries by applying low pressures at ambient temperature, *J. Eur. Ceram. Soc.*, 2005, vol. 25, p. 3403.
10. Timurkutluk, B., The role of lamination conditions on electrochemical and mechanical performance of ceramic electrolytes for solid oxide fuel cells, *Ceram. Int.*, 2015, vol. 41, p. 2057.
11. Capdevila, X.G., Folch, J., Calleja, A., et al., High-density YSZ tapes fabricated via the multi folding lamination process, *Ceram. Int.* 2009, vol. 35, p. 1219.
12. Park, H.-G., Moon, H., Park, S.-C., et al., Performance improvement of anode-supported electrolytes for planar solid oxide fuel cells via a tape-casting/lamination/co-firing technique, *J. Power Sources*, 2010, vol. 195, p. 2463.
13. Lee, S.-H., Messing, G.L., and Awano, M., Sintering arches for co-sintering camber-free SOFC multilayers, *J. Am. Ceram. Soc.*, 2008, vol. 91, p. 421.
14. Agarkov, D.A., Bredikhin, S.I., Burmistrov, I.N., Kuritsyna, I.E., Nepochatov, Yu.K., and Tiunova, O.V., *Membrana tverdogo elektrolita dlya tverdookisnykh toplivnykh elementov* (Solid Electrolyte Membrane for Solid Oxide Fuel Cells), RF Patent 161024, 2016.
15. Goulart, C. and de Souza, D., Critical analysis of aqueous tape casting, sintering, and characterization of planar yttria-stabilized zirconia electrolytes for SOFC, *Int. J. Appl. Ceram. Technol.*, 2017, p. 1.

Translated by L. Smolina